Staticand dynamic behaviour of flax–epoxy composites

Zheng He, Xiaoyu Sun [a, *], Xuan Gu, Qingbo Sui, Ju Liu, Kuo Yuan

College of Aerospace and Civil Engineering, Harbin Engineering University, Harbin 150001 China

[a]sunxiaoyu520634@163.com

Abstract

The present study focuses on the characterisation and evaluation of the fatigue behaviour of flax–epoxy composites. A better understanding of this behaviour allows the prediction of long-term properties to assess the viability and long-term durability of these materials. The purpose of this work is to systematically compare the tension–tension fatigue behaviour of flax fibre composites for one random mat, six textile architectures and two laminate configurations, which are used in a wide range of applications. The fibre architecture was found to have a strong effect on the fatigue behaviour, where higher static strength and modulus combinations present the best fatigue characteristics. They have a delayed damage initiation and increased fatigue life as well as a reduced damage propagation rate combined with higher energy dissipation in the early stages of fatigue loading.

Keywords

A. Fabrics/textiles; A. Biocomposites; B. Fatigue; B. Mechanical properties.

1. Introduction

Liang et al. [1] have found out that non-crimp glass fibre/epoxy composites have an increased resistance to fatigue loading compared to non-crimp flax/epoxy composites which, both having a [0, 90]3s lay-up, is due to their higher static strength (380 MPa vs ≈170 MPa). On the other hand, for the same lay-up, the glass composites have a larger reduction in fatigue life illustrated by a steeper specific *S–N* curve, in comparison to flax/epoxy, 56.2 MPa/decade vs 25.2 MPa/decade (which corresponds to a decrease of 15% of the ultimate

tensile strength (UTS) per decade for both of them) as seen in Fig. 1. This demonstrates a more steady fatigue behaviour through time for the flax/epoxy composite. Silva et al. [2] have shown that for technical sisal fibres (one fibre), at fatigue stresses below 50% of the ultimate tensile strength (UTS), all fibres resist more than 106 cycles. Furthermore, the authors have observed a slight increase in stiffness during the early cycles. A study published in 2014 by Shahzad and Isaac [3] showed that short hemp fibre random mat composites were less fatigue sensitive than the glass fibre chopped strand mat counterpart in tension–tension fatigue, which could be related to the lower stiffness degradation at equal normalised stress levels (*S*/*S*o). When the fibre architecture is varied, Shah et al. [4] found that increasing off-axis loading angle may improve the fatigue life at high loading rate (90% of the UTS). A steeper *S–N* curve (faster degradation) was observed for the [±45]4 F50/polyester laminate in comparison to unidirectional composite ([0]4) laminate and the [90]4. Tension–tension fatigue tests results from the same author showed that the textile architectures with fibre orientations off-axis to the loading direction resulted in lower fatigue properties, which is in line with the significant drop in composite static strength in those off-axis directions.

The aim of this study is to investigate *S–N* diagrams constructed from fatigue data at stress ratios of $R = 0.1$ (tension–tension) at various stress levels for nine different flax textile architectures combined with an epoxy matrix. The composites were manufactured via the resin transfer moulding process. The samples were then cut and mechanically tested in tensile direction to obtain the required ultimate tensile strength value, needed for the determining the stress levels during the fatigue testing. Strain monitoring was used during fatigue testing in order to assess the stiffness degradation rates as well

as the hysteresis loops. These data were also used to investigate the energy dissipation capability and the gradual build-up of the permanent strain of each material. The post-fatigue properties are also evaluated in order to assess the degradation rate of the composite through time. This investigation is crucial in order to understand the damage state, the post fatigue properties and fatigue life. This information will help to assess the durability of these types of composite materials, since these properties have a great influence on the service life, product safety and liability.

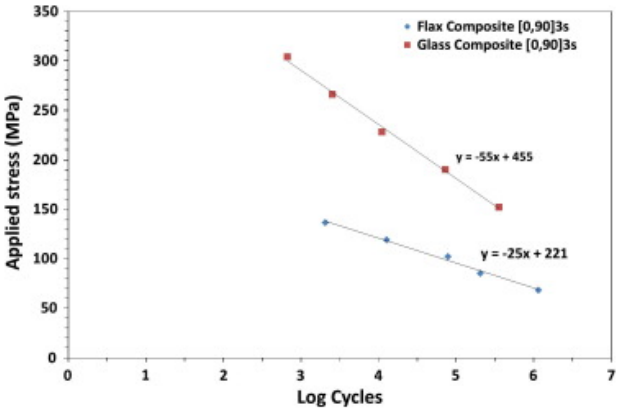

Fig. 1. *S–N* curves of [0, 90]3s cross ply flax/epoxy and glass/epoxy composites adapted from [2]. (For interpretation of the references to colour in this figure legend, the reader is referred to the web version of this article.)

2. Experimental

The flax fibre reinforced composites were made by combining a thermoset epoxy matrix with nine flax textile configurations. For the cross-linking, the matrix *Epikote 828LVEL* (viscosity$\eta \approx 10–12$ Pa s at 25 °C) is mixed with the hardener *Dytek DCH-99* at a 15.2 phr ratio. The 2 mm thick laminates are composed of several layers of fabrics in order to obtain a fibre volume fraction (Vf) of ≈40%, except for the random mat composite which has a $Vf \approx 30\%$. The tensile stiffness is calculated in two distinct regions, $E1$ between 0% and 0.1% strain and $E2$ between 0.3% and 0.5% strain as displayed in Fig. 2. The motivation for calculating two values for the stiffness is because of a typical decrease in stiffness for these materials around 0.2% strain in flax fibres which is observed for all the studied configurations. The decrease rate (strain softening) will depend on the type of preform used in the composite. The more fibre-dominated behaviour, the more the softening will be visible which has to be taken into account while analysingFig. 3(a). It is thus important to mention both values, as they both are relevant for design purposes.

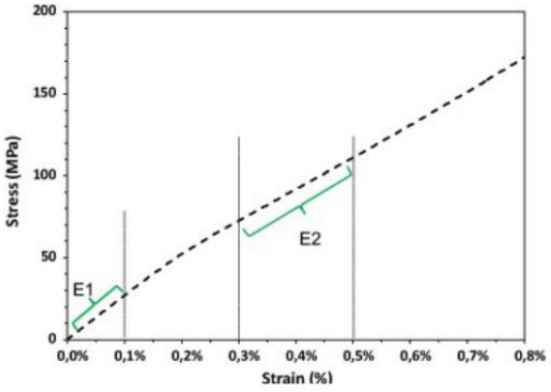

Fig. 2. Zones where the moduli $E1$ and $E2$ are calculated. (For interpretation of the references to colour in this figure legend, the reader is referred to the web version of this article.)

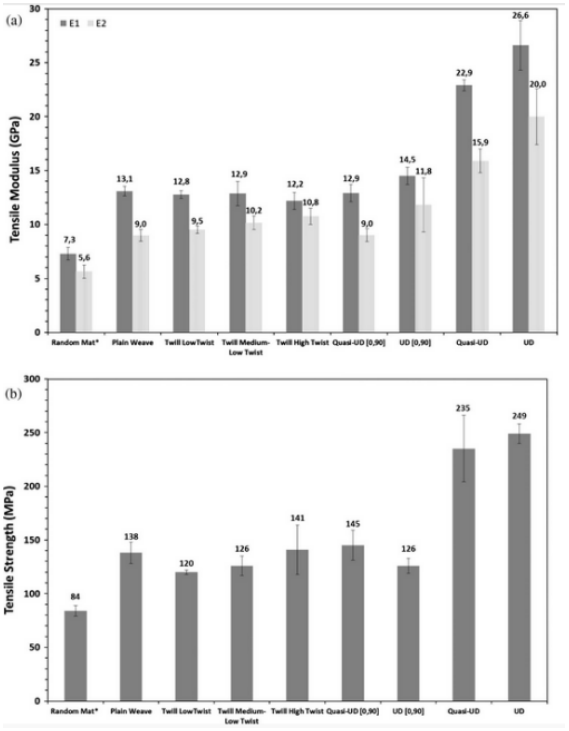

Fig. 3. (a) the *E*1 and *E*2 moduli and (b) the ultimate tensile strength for the investigated flax/epoxy composites.

Later on, the fatigue tests were conducted in temperature-controlled laboratory at 21 °C using UTS data from Fig. 3(b). A tapered sine signal, as displayed in Fig. 4(a), was applied to gradually build up the load amplitude and avoid an overshoot of the load during the early cycles. Samples were prepared with the same dimensions as for static tensile testing and end-tabbed. The test is set to stop if the samples do not fail after 106 cycles, referred to as *N*max. Hysteresis loops and stiffness degradation were captured continuously using a fatigue rated extensometer with a gauge length of 50 mm. The dynamic stiffness during cycling was measured in the first part of the loading curves of each hysteresis loop as shown in Fig. 4(b). A minimum of 4 samples for each stress level was used.

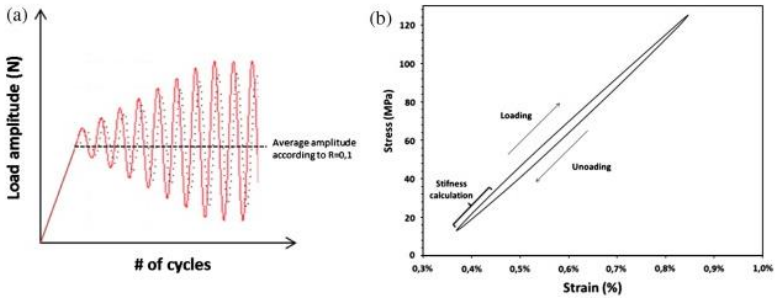

Fig. 4. (a) Tapered sine signal used for fatigue cycling and (b) calculation of the dynamic stiffness from the loading curves of the hysteresis loop for monitoring of the stiffness degradation. (For interpretation of the references to colour in this figure legend, the reader is referred to the web version of this article.)

3. Results And Discussion

Tensile–tensile fatigue cycling was carried out at maximum stress levels corresponding to various fractions of the UTS registered during quasi-static testing. This value of UTS is referred to as *S*o, and it is later used to normalise the maximum stress levels that the samples are subjected to (*S*/*S*o). Fig. 5 presents a global, and hence rather crowded overview of the *S*–*N* curves, describing the fatigue life of the nine chosen flax/epoxy configurations.

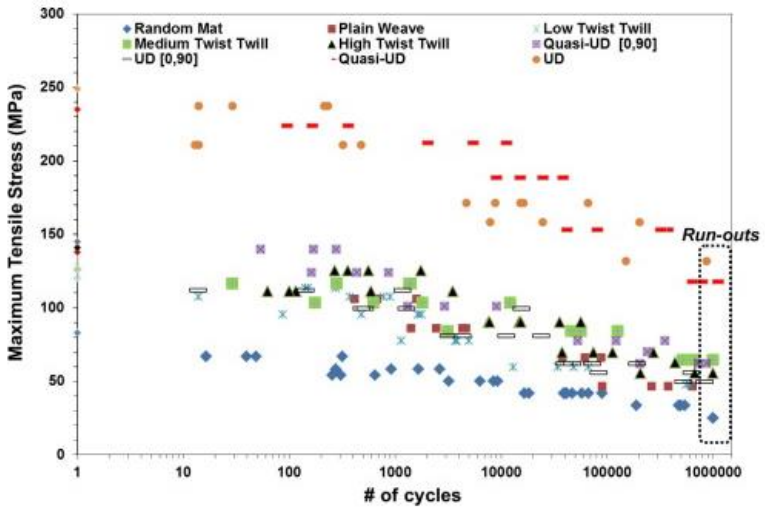

Fig. 5. Stress-life data for untreated flax–epoxy composites at R = 0.1 (including static strengths values). (For interpretation of the references to colour in this figure legend, the reader is referred to the web version of this article.)

To compare the fatigue sensitivity of the studied materials, the normalised stress (S/So) versus cycles to failure (N) curve method is used (see Fig. 6). The normalised curves show that the fatigue strength of the different composites at high stress level (S/So = 0.9 and 0.8) is rather scattered, and that the data points for the different reinforcement architectures overlap. At these higher stress levels, the fatigue strength steadily decreases, per decade of cycles, by an average of 5–10% of the static strength. A similar value of static strength reduction was reported by Mandell and Meier [5] and Shazad and Isaac [3] for UD E-glass fibre and randomly oriented hemp fibre reinforced composites respectively, which means that natural fibre composites demonstrate comparable fatigue sensitivity as unidirectional glass fibre composites [6].

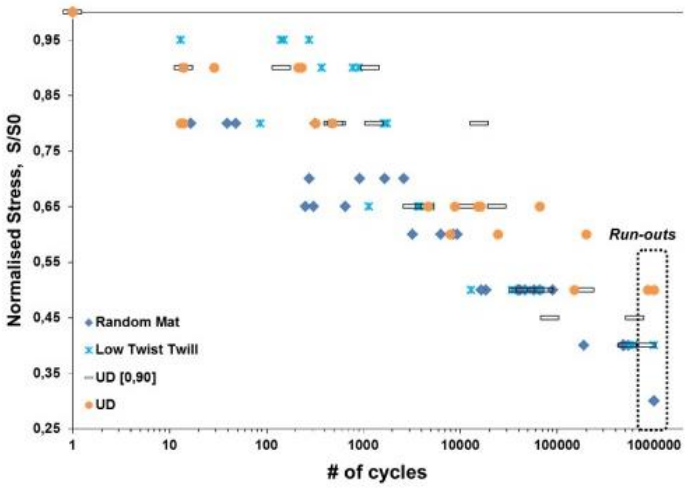

Fig. 6. Normalised fatigue data for flax–epoxy composites at R = 0.1. (For interpretation of the references to colour in this figure legend, the reader is referred to the web version of this article.)

The trendlines, calculated for data points of the normalised stresses S/So vs the number of cycles to failure, presented in Fig. 7, show a clear difference. The endurance limit of the UD composite clearly exceeds the ones of the Low Twist Twill, the cross-ply laminate as well as the random mat. Its endurance limit is 50% of the UTS, while for the UD [0, 90] cross-ply laminate and for the Low Twist Twill it drops to 35% of the UTS and for the random mat even to 30%. All the slopes show dissimilar trends, with the Low Twist Twill showing the highest degradation with time, due to its weaving pattern characteristics and yarn type (see Fig. 13).

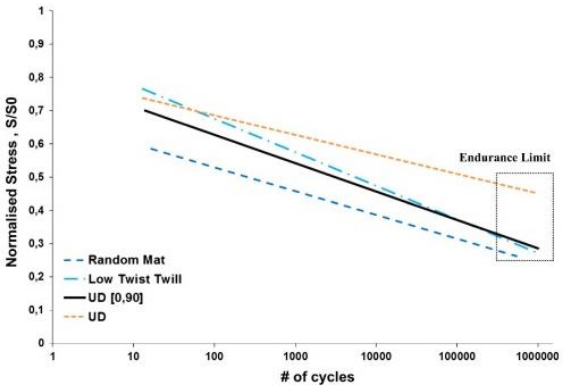

Fig. 7. Normalised fatigue data trendlines for four flax–epoxy composites at $R = 0.1$. (For interpretation of the references to colour in this figure legend, the reader is referred to the web version of this article.)

In the early cycles, defined as Region I in Fig. 9, an increase in stiffness is observed. This could be related to the reorientation of the microfibrils in the elementary fibre observed by several researchers. This could however be counteracted by some damage initiation as the microfibrils rotate towards the loading direction (0°)[1-3].For the 90° layer in a crossply laminate, the constraint of the 0° ply is also present[7]. Thus, the laminate failure will not be caused by only a crack in the 90°-ply, but by shear-lag creating delaminations in between the 0° and 90° plies causing a gradual stiffness decrease as illustrated in Fig. 8. For flax composites, the interlaminar fracture toughness is higher compared to carbon or glass composites, which limits the propagation of delaminations, thus limiting the stiffness degradation [8]. On the other hand, no indication of imminent failure is given and the flax composites will tend to fail catastrophically due to the coalescence of cracks [3] ; [9].

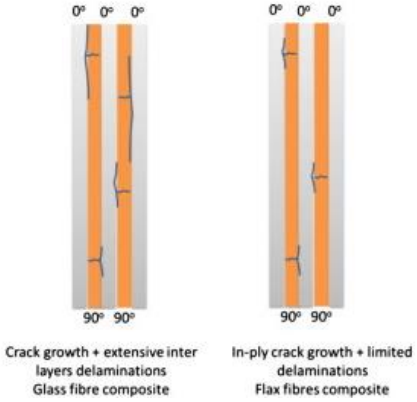

Fig. 8. Crack propagation in a [0, 90] cross ply laminate. (For interpretation of the references to colour in this figure legend, the reader is referred to the web version of this article.)

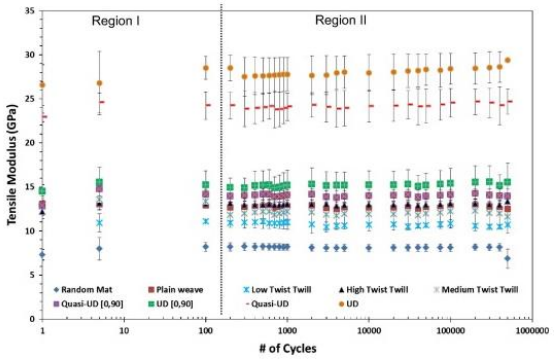

Fig. 9. Stiffness degradation curves at $S/So = 0.3$. (For interpretation of the references to colour in this figure legend, the reader is referred to the web version of this article.)

The samples exposed to fatigue cycling up to 500,000 cycles were tested in static tension to determine their residual properties. The moduli *E*1 and *E*2, and the ultimate tensile strength were determined and are presented in Fig. 12. The post-fatigue tensile tests show that the fatigue-tested samples exhibit similar properties to the static-tested samples with no significant decrease in mechanical properties. The same behaviour was observed with hemp fibre based composites by Shahzad and Isaac [3].Taking a closer look at the results (is presented in Fig. 12), a moderate increase of the *E*1moduli is observed for the Quasi-UD [0, 90] by +5%, the UD [0, 90] with 10%, whereas the*E*1-moduli for the quasi-UD (+0.5%) and UD composites (+2.5%) remain almost constant. A different behaviour is observed for their *E*2 modulus with stable behaviour (UD [0, 90] or an increased modulus up to 25% for the Quasi-UD [0, 90). For the previous laminates, all the strength values decrease compared to the static value, besides the UD [0, 90] being the most stable composite configuration. By looking at the stress–strain curves before and after fatigue (seen in Fig. 12(d)), a change in the non-linear behaviour was observed. For the plain weave and high twist twill architecture, as the yarns are wet spun, the water dissolves the pectin which leads to partial or full separation of the elementary fibres (fibrillation) present in the yarns as seen in Fig. 11.

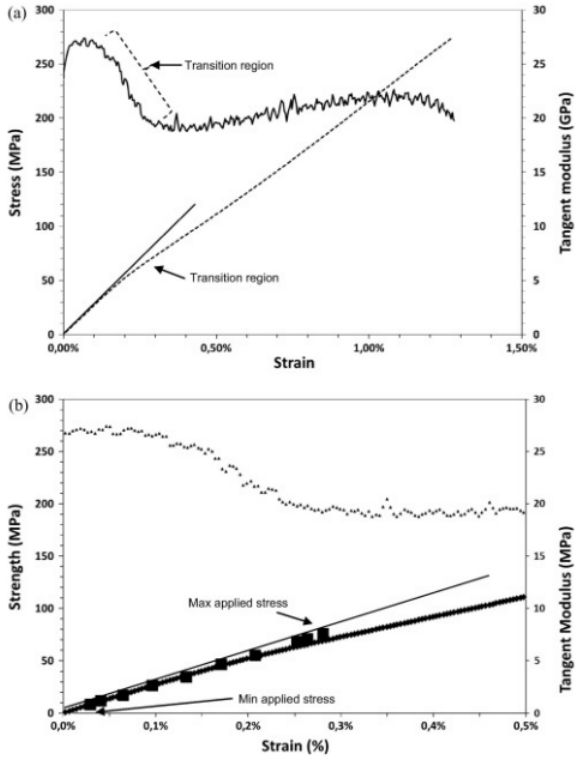

Fig. 10. (a) Position of the transition region in a static tensile test and the fatigue testing range at 30% of the UTS and (b) zoom in to showcase behaviour at low strains. Example for the UD configuration.

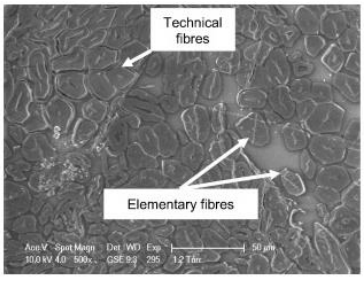

Fig. 11. Micrograph of the plain weave/epoxy composite showing the fibrillation of the elementary fibres due to wet spinning.

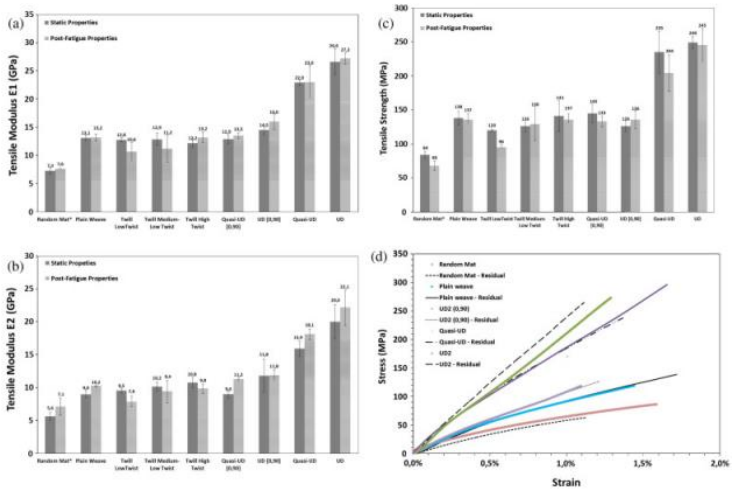

Fig. 12. Post fatigue properties of flax–epoxy composite, (a) the tensile modulus *E*1, (b) the tensile modulus *E*2, (c) the tensile strength and (d) selection of stress–strain curve before and post-fatigue (residual) testing. (For interpretation of the references to colour in this figure legend, the reader is referred to the web version of this article.)

As the applied stress is 30% of the UTS and $R = 0.1$, the cycling goes from a minimum stress in the linear elastic region to a maximum stress in the transition zone, as observed in a static tensile test (see Fig. 2), this is once more displayed by the dotted line in Fig. 10(b) (■). Thus, the specimens are loaded into the "visco-elasto-plastic region". This leads to a permanent deformation, which can be related to plastic deformation but not necessarily to damage. This permanent deformation can be seen in Fig. 14 showing an increase of the strain at the minimum stress as a function of the number of cycles.

Fig. 13. Unidirectional flax roving with binding polyester yarn in the low twist twill textile. (For interpretation of the references to colour in this figure legend, the reader is referred to the web version of this article.)

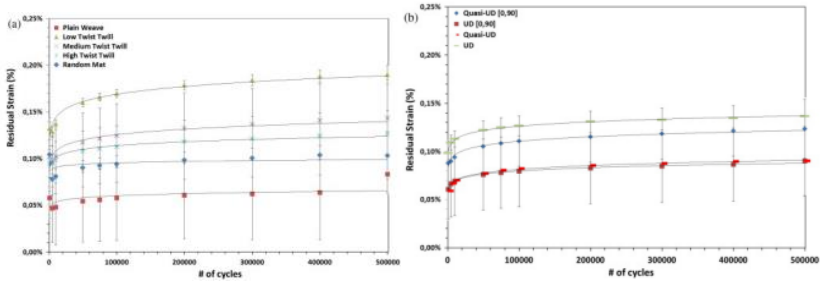

Fig. 14. Permanent deformation through cycling. Display of the minimum strain level reached by the hysteresis during fatigue cycling at a stress level of *S*/*So* = 0.3: (a) random mat and woven composites and (b) [0, 90] cross-ply laminate and unidirectional composites. (For interpretation of the references to colour in this figure legend, the reader is referred to the web version of this article.)

This can be seen in Fig. 15. Where the samples were tested at a higher stress level (50% of UTS). The shift of the hysteresis loop towards increasing strain levels is an indication of permanent deformation of the specimen [7]. Additionally, a larger stress–strain (σ–ε) hysteresis loop area and an

slight increase of the slope in the early cycles compared to cycles close to the failure of the sample was observed for four of the nine architectures (seeFig. 15).

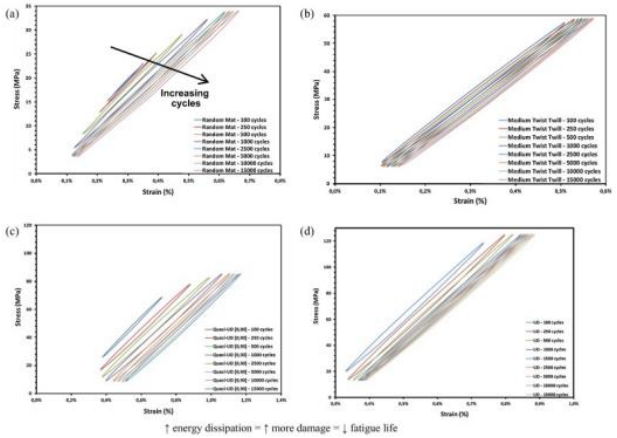

Fig. 15. Stress–strain data from fatigue testing for the first 15,000 cycles for (a) random mat, (b) medium twist twill, (c) quasi-UD [0, 90] and (d) UD composites at *S*/*S*o = 0.5. (For interpretation of the references to colour in this figure legend, the reader is referred to the web version of this article.)

For the plain woven-based composites, the cracks may have grown at the warp and weft yarns crossovers, as seen in Fig. 16(a) and the inter-layer delamination was most probably caused by out-of-plane shear stress. The crack propagation from the weft direction through matrix cracking was also found by Jacobsen and Brøndsted [10] for plain woven carbon composites. In Fig. 16(b), the failure mainly happens at the yarn-matrix interface with extensive fibre pull-out where the crack runs around the yarns.For the random mat composite shown in Fig. 16(c) and (d), fibre matrix debonding is the main failure mode combined with fibre pull out. Long river-like shape crack features can be seen in the SEM image, where at the fibre debonded from the matrix. Besides the extensive evidence of fibre pull-out, fibre failures were also observed. As the fibres are oriented in all directions, a mixed failure mode is observed.For the unidirectional composites, Fig. 16(e) and (f), displays a homogenous distribution of the fibres.

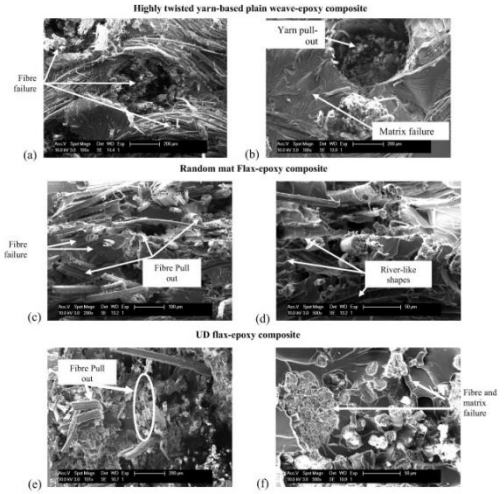

Fig. 16. SEM images of flax–epoxy composites of highly twisted yarn-based plain weave composite after fatigue cycling: (a) damage at the yarn warp and weft crossover and (b) yarn pull out. SEM images of flax–epoxy random mat composite after fatigue cycling: (c) pull-out and fibre failure and (d) fibre–matrix debonding (arrows) and the SEM images of flax–epoxy UD composite after fatigue cycling: (e) fibre matrix interface failure (arrows) and (f) fibre and matrix failure.

4. Conclution

Overall, the behaviour of flax–epoxy composites is comparable to glass fibre reinforced composites in the literature and thus suitable for many new or existing industrial applications. Further optimisation of composites lay-up and combination with suitable matrices, need to be made. One of the target would be to increase the fibre/matrix interface bonding, which may increase the mechanical and the fatigue properties. Finally, the damage evolution could be quantified using the information from the hysteresis loops to assess the energy dissipation.

Acknowledgements

This work is supported by the National Natural Science Foundation of China（No. 11602066） and the National Science Foundation of Heilongjiang Province of China (QC2015058 and 42400621-1-15047), the Fundamental Research Funds for the Central Universities.

References

[1] S. Liang, P.B. Gning, L. Guillaumat A comparative study of fatigue behaviour of flax/epoxy and glass/epoxy composites Compos Sci Technol, 72 (5) (2012), pp. 535–543
[2] Fd.A. Silva, N. Chawla, R.D. de Toledo Filho An experimental investigation of the fatigue behavior of sisal fibers Mater Sci Eng, A, 516 (1–2) (2009), pp. 90–95
[3] A. Shahzad, D. Isaac Fatigue properties of hemp and glass fiber composites Polym Compos, 35 (10) (2014), pp. 1926–1934
[4] D.U. Shah, P.J. Schubel, M.J. Clifford, P. Licence Fatigue life evaluation of aligned plant fibre composites through S/N curves and constant-life diagrams Compos Sci Technol, 74 (2013), pp. 139–149
[5] Mandell JF, Meier U. Effects of stress ratio, frequency, and loading time on the tensile fatigue of glass-reinforced epoxy. Long-term behavior of composites, ASTM STP 813; 1983. p. 55–77.
[6] Shahzad A, Isaac D. Fatigue properties of hemp fibre composites. In: 17th International conference on composite materials (ICCM-17), Edinburgh, UK; 2009.
[7] K. Vallons, M. Zong, V. Lomov, I. Verpoest Carbon composites based on multi-axial multi-ply stitched preforms – Part 6. Fatigue behaviour at low loads: stiffness degradation and damage development Compos Part A – Appl Sci Manuf, 38 (7) (2007), pp. 1633–1645
[8] Y. Zhang, Y. Li, H. Ma, T. Yu Tensile and interfacial properties of unidirectional flax/glass fiber reinforced hybrid composites Compos Sci Technol, 88 (2013), pp. 172–177
[9] S. Giancane, F.W. Panella, V. Dattoma Characterization of fatigue damage in long fiber epoxy composite laminates Int J Fatigue, 32 (1) (2010), pp. 46–53
[10] T.K. Jacobsen, P. Brøndsted Mechanical properties of two plain-woven chemical vapor infiltrated silicon carbide-matrix composites J Am Ceram Soc, 84 (5) (2001), pp. 1043–1051